2-1-2015

A moonlighting function of Mycobacterium smegmatis Ku in zinc homeostasis?

Ambuj K. Kushwaha
Louisiana State University

Dinesh K. Deochand
Louisiana State University

Anne Grove
Louisiana State University

Recommended Citation

Kushwaha, A., Deochand, D., & Grove, A. (2015). A moonlighting function of Mycobacterium smegmatis Ku in zinc homeostasis?. *Protein Science, 24* (2), 253-263. https://doi.org/10.1002/pro.2612

THE PROTEIN SOCIETY

A moonlighting function of *Mycobacterium smegmatis* Ku in zinc homeostasis?

Ambuj K. Kushwaha, Dinesh K. Deochand, and Anne Grove*

Department of Biological Sciences, Louisiana State University, Baton Rouge, Louisiana 70803

Received 7 August 2014; Accepted 25 November 2014
DOI: 10.1002/pro.2612
Published online 28 November 2014 proteinscience.org

ABSTRACT: Ku protein participates in DNA double-strand break repair via the nonhomologous end-joining pathway. The three-dimensional structure of eukaryotic Ku reveals a central core consisting of a β-barrel domain and pillar and bridge regions that combine to form a ring-like structure that encircles DNA. Homologs of Ku are encoded by a subset of bacterial species, and they are predicted to conserve this core domain. In addition, the bridge region of Ku from some bacteria is predicted from homology modeling and sequence analyses to contain a conventional HxxC and CxxC (where x is any residue) zinc-binding motif. These potential zinc-binding sites have either deteriorated or been entirely lost in Ku from other organisms. Using an *in vitro* metal binding assay, we show that *Mycobacterium smegmatis* Ku binds two zinc ions. Zinc binding modestly stabilizes the Ku protein (by ~3°C) and prevents cysteine oxidation, but it has little effect on DNA binding. *In vivo*, zinc induces significant upregulation of the gene encoding Ku (~sixfold) as well as a divergently oriented gene encoding a predicted zinc-dependent MarR family transcription factor. Notably, overexpression of Ku confers zinc tolerance on *Escherichia coli*. We speculate that zinc-binding sites in Ku proteins from *M. smegmatis* and other mycobacterial species have been evolutionarily retained to provide protection against zinc toxicity without compromising the function of Ku in DNA double-strand break repair.

Keywords: DNA binding; Ku protein; MarR; PAR assay; thermal stability; zinc binding

Introduction

Ku protein is an important component of the nonhomologous end-joining (NHEJ) pathway of DNA double-strand break repair, and it is ubiquitous among eukaryotes.[1–5] Some bacterial species encode a homolog of Ku, and bacterial Ku proteins function along with a dedicated ligase to repair DNA double-strand breaks and protect against genome rearrangements (for review, see Ref. 6). The overall three-dimensional topology of Ku is predicted to be conserved from prokaryotes to eukaryotes although the protein sequence has diverged significantly during the course of evolution. Eukaryotic Ku proteins are heterodimers consisting of Ku70 and Ku80, whereas the 30–40 kDa prokaryotic Ku proteins are homodimers and composed of just the DNA-binding core domain of eukaryotic Ku.[1,4,5,7] The structure of

Abbreviations: DTNB, 5,5′-dithiobis-(2-nitrobenzoic acid); DTT, dithiothreitol; EDTA, ethylenediaminetetraacetic acid; EMSA, electrophoretic mobility shift assay; NHEJ, nonhomologous end-joining; PAR, 4-(2-pyridylazo) resorcinol.

Additional Supporting Information may be found in the online version of this article.

Ambuj K. Kushwaha's current address is Laboratory of Malaria and Vector Research, National Institute of Allergy and Infectious Diseases, Rockville, Maryland 20852.

Grant sponsor: The National Science Foundation; Grant number: MCB-1051610; Grant sponsor: LSU Economic Development Assistantship.

*Correspondence to: Anne Grove, Department of Biological Sciences, Louisiana State University, Baton Rouge, LA 70803, Tel.: +1–225-578–5148, Fax: +1–225-578–8790.
E-mail: agrove@lsu.edu

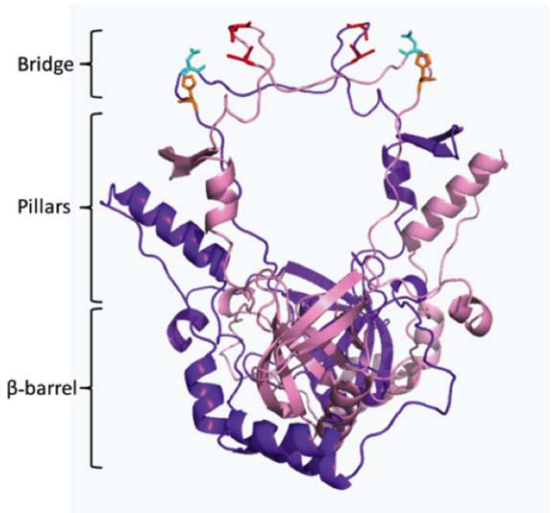

Figure 1. Model of *M. smegmatis* Ku illustrating the predicted zinc-binding sites. Each monomer (in purple and light pink) is modeled on template strands 1jeyA and 1jeyB. The residues previously predicted to coordinate zinc are highlighted in different colors: cysteine (red), histidine (orange), and aspartic acid (cyan). The model was created using SwissModel in automatic mode. The image was prepared with PyMOL (www.pymol.org).

eukaryotic Ku70 and Ku80 subunits reveals three domains: an N-terminal domain, a central DNA-binding domain, and a C-terminal domain; the central core that consists of a β-barrel domain forms the base, pillar, and bridge regions that together form a ring-like structure through which DNA is threaded.[4,5,8] Ku makes few contacts to the phosphate backbone and participates in aligning broken DNA ends to promote end-joining. Homology modeling predicts that this DNA-binding domain is conserved in prokaryotic Ku proteins (Fig. 1).

Sequence analysis and homology modeling has previously suggested that the bridge-region of Ku from certain bacteria and their bacteriophages contains pairs of cysteine and histidine residues that may potentially form a conventional HxxC and CxxC (where x is any residue) zinc-binding site (Fig. 1).[9] In certain cases, the binding site is slightly modified with some cysteines being replaced by acidic residues, which can also participate in chelating zinc. Ku proteins with putative zinc-binding sites were identified in organisms belonging to firmicutes, actinobacteria, and their viruses, whereas these sites were seen to have either deteriorated or been entirely lost in Ku from other organisms.[9] It was suggested that the bridge-region of Ku is derived from a regular zinc-ribbon by a segment-swapping event, and that it belongs to a new family of zinc-ribbon folding domain.[9]

Intrigued by the *in silico* prediction of a zinc-binding motif in Ku proteins from actinobacteria, we tested the effect of zinc on *Mycobacterium smegmatis* Ku. We show that *M. smegmatis* Ku indeed binds zinc *in vitro*. *In vivo*, the exposure of *M. smegmatis* cultures to excess zinc results in significant upregulation of the *ku* gene, and *Escherichia coli* cells expressing *M. smegmatis* Ku have increased tolerance to zinc. Considering that zinc binding does not compromise the DNA-binding properties of Ku, we suggest a moonlighting function of Ku in protecting cells against zinc toxicity.

Results and Discussion

Ku binds zinc

A multiple sequence alignment of Ku proteins from Gram-positive bacteria such as *Bacillus* species show the conservation of potential zinc-binding motifs (i.e., HxxC and CxxC, where x is any residue), whereas Ku from Gram-negative bacteria such as *Pseudomonas* species entirely lack these putative zinc-binding sites (Fig. 2). Mycobacterial species also encode Ku with likely zinc-binding sites, however, with slight modifications, as one or more of the cysteine residues have been replaced by aspartic acid (Fig. 2). We therefore examined zinc binding by recombinant *M. smegmatis* Ku, which was expressed in *E. coli* using media without added zinc as described earlier.[10] As determined by gel filtration chromatography, *M. smegmatis* Ku exists as the expected dimer in solution.[10] The cysteines identified as part of the potential zinc-binding motif are the only cysteines in the protein.

To assess the ability of *M. smegmatis* Ku to bind zinc *in vitro*, we used 4-(2-pyridylazo) resorcinol (PAR), which is a metallochromic chelator that forms complex with various divalent metals, resulting in a diagnostic absorbance of the metal–PAR complex. The uncomplexed PAR has an absorbance maximum at 416 nm, however, when complexed with zinc its absorbance at 500 nm increases significantly. The following Ku samples were analyzed by the measurement of absorbance after the incubation of PAR with protein: Zinc-free native Ku (His_6-tagged Ku expressed in *E. coli* without added zinc and purified in the presence of ethylenediaminetetraacetic acid [EDTA]); zinc-bound native Ku (His_6-tagged native Ku incubated with Zn^{2+}, followed by dialysis to remove unbound metal); denatured zinc-free Ku (zinc-free native Ku denatured by heating in the presence of SDS); and denatured zinc-bound Ku (zinc-bound native Ku subsequently denatured by heating in the presence of SDS).

No change in the wavelength of PAR absorbance was observed on addition of zinc-free native Ku (Fig. 3(A), gray line) or denatured zinc-free Ku (Fig. 3(B), gray line), suggesting that Ku purified from *E. coli* has no metal bound, possibly owing to low affinity and/or the presence of EDTA (metal chelator) in the purification buffer. However, a significant increase

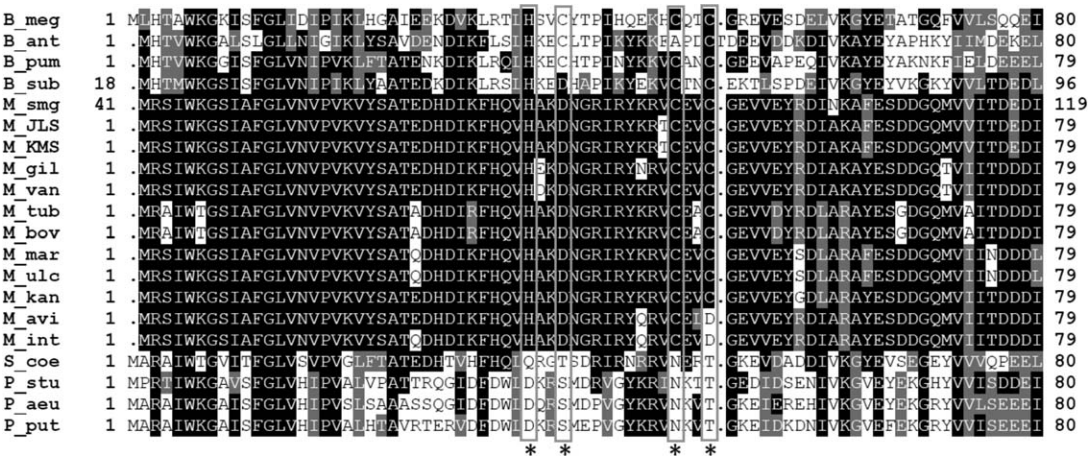

Figure 2. Multiple sequence alignment of bacterial Ku homologs. The first and last residue numbers are indicated before and after each sequence in the alignment. Positions corresponding to zinc-binding residues are boxed and marked by asterisks below the alignment. B_meg, *Bacillus megaterium*; B_ant, *Bacillus anthracis*; B_pum, *Bacillus pumilus*; B_sub, *Bacillus subtilis*; M_smg, *Mycobacterium smegmatis*; M_JLS, *Mycobacterium* Sp. JLS; M_KMS, *Mycobacterium* Sp. KMS; M_gil, *Mycobacterium gilvum*; M_van, *Mycobacterium vanbaalenii*; M_tub, *Mycobacterium tuberculosis*; M_bov, *Mycobacterium bovis*; M_mar, *Mycobacterium marinum*; M_ulc, *Mycobacterium ulcerans*; M_kan, *Mycobacterium kansasii*; M_avi, *Mycobacterium avium*; M_int, *Mycobacterium intracellulare*; S_coe, *Streptomyces coelicolor*; P_stu, *Pseudomonas stutzeri*; P_aeu, *Pseudomonas aeruginosa*; P_put, *Pseudomonas putida*.

in the absorbance at 500 nm was seen when PAR was incubated with zinc-bound native Ku or denatured zinc-bound Ku (Fig. 3(A,B), black lines). Ku protein was purified with an N-terminal His_6-tag and hence to rule out the possibility of the His_6-tag binding zinc, the PAR assay was performed with Ku protein in which the His_6-tag was cleaved by enterokinase (Supporting Information Fig. S1). Again, a significant increase in absorbance maximum at 500 nm was seen when the PAR assay was performed with zinc-bound native and denatured Ku (Fig. 3(A,B), dashed lines). Thus, a comparable increase in absorbance at 500 nm is observed on incubation of PAR with both native and denatured zinc-bound Ku, which indicates efficient release of Zn^{2+} from native Ku, likely reflecting that Ku has a lower affinity for zinc compared to PAR (for which the pH-dependent dissociation constants are in the μM range, corresponding to a β_{PAR} of 2.2×10^{12} at pH 7.0.)[11] Titrating His_6-tagged Ku into a solution of PAR_2Zn (containing excess PAR to ensure complete conversion to the PAR_2Zn complex) shows that Ku does compete with PAR for zinc binding, with an estimated apparent $K_d = 0.8 \pm 0.3$ nM (Fig. 4).

The higher absorbance of PAR incubated with non-His_6-tagged zinc-bound native Ku (Fig. 3(A), dashed line) as compared to His_6-tagged zinc-bound native Ku (Fig. 3(A), black line) is unexpected; this difference in absorbance is also seen under denaturing conditions (Fig. 3(B); considering the baseline shift on addition of SDS). If both the tag and the zinc-binding site in Ku-bound zinc, then the expectation would be for the greatest zinc release from tagged protein. Zinc release from His_6-tagged Ku is consistently and reproducibly lower than zinc release from Ku in which the tag is removed, which leaves us with the inference that the tag interferes with zinc binding to the zinc-binding site in Ku, perhaps by the flexible tag moving toward the putative zinc sites, and hence creating a "hybrid" site to which zinc binds with lower affinity, resulting in lower occupancy. The reason for the lower zinc release from His_6-tagged protein notwithstanding, the release of zinc from untagged protein demonstrates that Ku does bind zinc.

The stoichiometry of zinc to protein was estimated by the PAR assay.[12] To ensure the quantitative release of metal from zinc-bound Ku (without its His_6-tag), the protein was denatured by heating in the presence of SDS. The released zinc was detected by PAR, which binds Zn^{2+} in a 2:1 ratio,[13] and the amount of zinc bound per Ku molecule was estimated by comparison with a Zn^{2+} standard curve (Supporting Information Fig. S2). It was estimated that 0.5 μM of monomeric Ku protein bound 0.47 μM of Zn^{2+}, which would correspond to dimeric Ku binding 1.88 zinc atoms. This is consistent with the predicted presence of two zinc sites per Ku dimer.

To address specifically the role of cysteine residues in zinc coordination, we simultaneously replaced both cysteines at positions 88 and 91 with alanine to generate KuC8891A (Supporting Information Fig. S1B). Contrary to our expectation, PAR assay with zinc-bound KuC8891A revealed an increase in absorbance at 500 nm [Fig. 3(C)], which indicates that disruption of the predicted zinc-binding motif does not abolish zinc binding. One

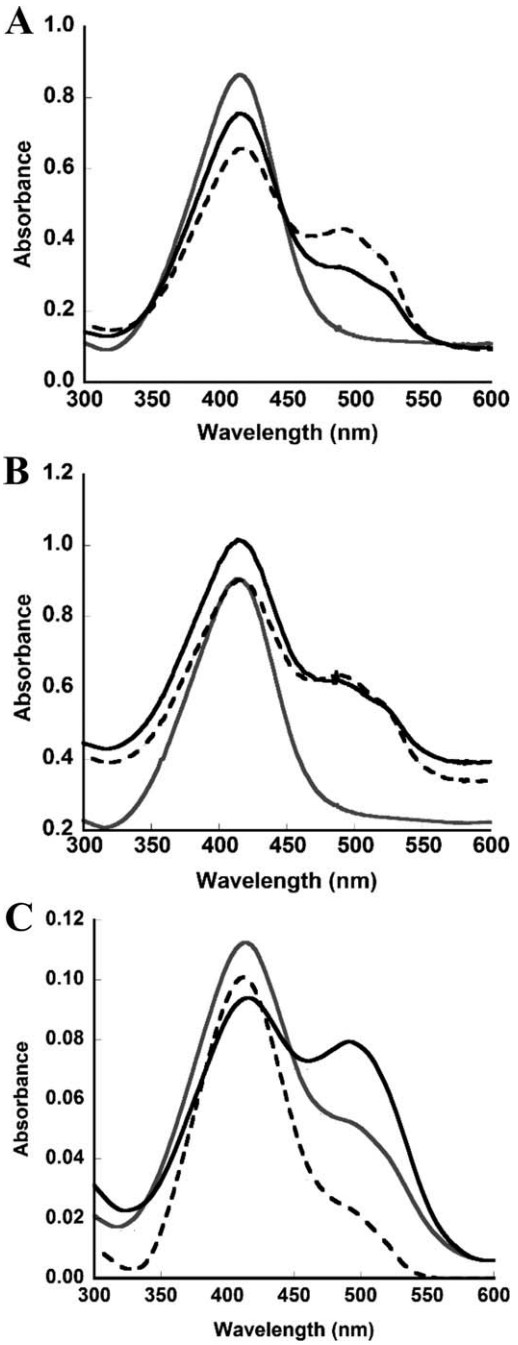

Figure 3. Zinc binding by Ku. Release of zinc from Ku monitored by its complexation with PAR, resulting in a diagnostic absorbance at 500 nm; uncomplexed PAR has an absorbance maximum at 416 nm. (A) Zinc release from native Ku. Absorbance spectrum of zinc-free native Ku (gray line); zinc-bound native Ku (black line); zinc-bound native Ku without His_6-tag (dashed line). (B) Zinc release from denatured Ku. Denatured zinc-free Ku (gray line); denatured zinc-bound Ku (protein denatured after incubation with zinc; black line); denatured zinc-bound Ku without His_6-tag (dashed line). Denaturation by SDS resulted in an overall increase in the baseline. (C) Zinc release from KuC8891A. Absorbance spectrum of PAR (dashed line); denatured KuC8891A (gray line); denatured zinc-bound KuC8891A (black line).

interpretation of this result would be that zinc binding to *M. smegmatis* Ku occurs at a site distinct from that of previously predicted. For example, glutamate residues at position 89, 93, or 96 within the DNA-encircling loop might participate in such zinc coordination (indeed, the alternate metal-binding site in KuC8891A may not even involve H75 and D78 predicted to participate in the originally predicted zinc site).

Zinc stabilizes Ku

When structural zinc sites in globular proteins are occupied, a large increase in thermal stability is commonly observed compared to the apo form of the protein. However, the predicted zinc site in Ku is not expected to induce or stabilize secondary structures as it resides in the flexible bridge region that encircles DNA. Instead, zinc coordination would be expected to link and perhaps reduce flexibility of the DNA-binding loops of two Ku monomers. To assess the effect of zinc binding on Ku protein stability, the thermal stability of zinc-free native Ku, bipyridyl-treated native Ku, and zinc-bound native Ku was compared using SYPRO Orange as a fluorescent reporter of protein unfolding (Fig. 5). The melting temperature (T_m) of untreated zinc-free native Ku and bipyridyl-treated native Ku was identical with T_m of 44.3 ± 0.3°C [Fig. 5(A)] and 44.3 ± 0.2°C [Fig. 5(B)], respectively, in accordance with the inference from PAR–chelation experiments that Ku isolated from *E. coli* has no metal bound. However, zinc-bound native Ku had a T_m of 47.1 ± 0.1°C [Fig. 5(C)], indicating a role for zinc in stabilizing the protein. The relatively modest increase in thermal stability is consistent with the stabilization of the flexible loops responsible for encircling DNA as

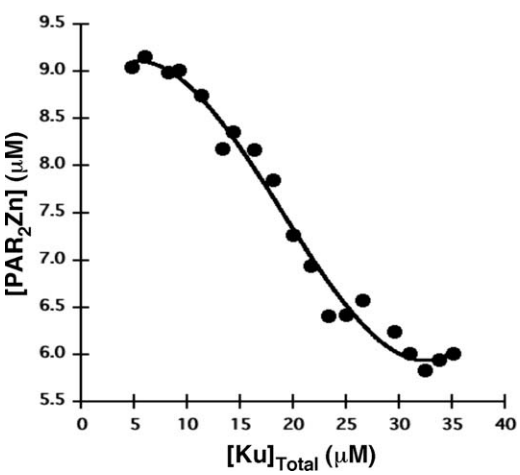

Figure 4. Affinity of Ku for zinc. Concentration of PAR_2Zn, calculated based on the absorbance at 500 nm, as a function of added protein. His_6-tagged protein was titrated into a solution of 210 μ*M* PAR and 10 μ*M* $ZnCl_2$. An apparent K_d of 0.8 ± 0.3 n*M* was estimated. A representative experiment is shown.

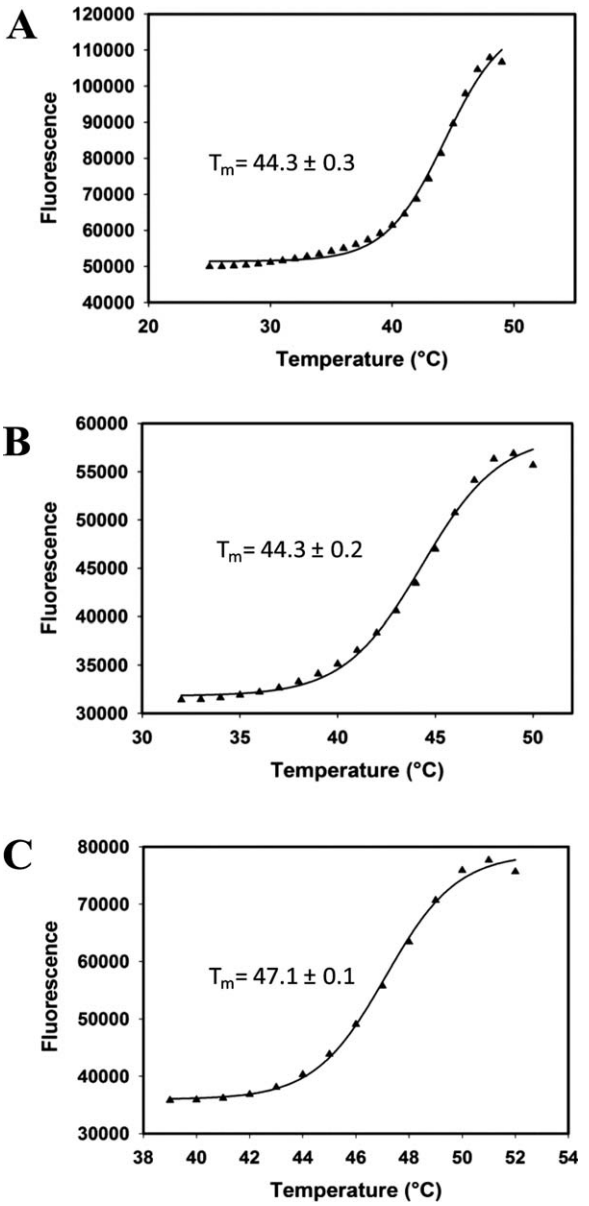

Figure 5. Melting temperature determination by differential scanning fluorimetry. Fluorescence of SYPRO Orange bound to exposed hydrophobic protein regions as a function of temperature. (A) Thermal denaturation curve of zinc-free Ku. T_m (with S.D.) is 44.3 ± 0.3°C. (B) Thermal denaturation curve of bipyridyl-treated Ku. T_m (with S.D.) is 44.3 ± 0.2°C. C. Thermal denaturation curve of zinc-bound Ku. T_m (with S.D.) is 47.1 ± 0.1°C.

opposed to stabilization of the globular protein core. By comparison to regulatory ligand-binding sites, a change in thermal stability of ~3°C on ligand binding is considered significant.[14]

Cysteine participates in zinc coordination

While the stoichiometry of zinc binding to Ku supports the presence of two binding sites, and the modest increase in thermal stability on zinc binding is consistent with binding to the DNA-binding loops, substitution of cysteines does not abolish zinc binding. To determine if cysteine residues do participate in zinc binding, we first assessed if zinc binding prevents cysteine oxidation. The effect of oxidizing and reducing agents on zinc-free native Ku and zinc-bound native Ku was first analyzed by SDS-PAGE. Reduced zinc-free Ku or bipyridyl-treated Ku migrated near the 55.6 kDa marker (Fig. 6(A), lanes 2 and 4). Both untreated zinc-free Ku and bipyridyl-treated Ku formed a higher molecular weight oligomeric species with a molecular weight of about 158 kDa when incubated with 10 m*M* of H_2O_2, and oxidized monomeric Ku consistently migrated slightly slower than reduced Ku (Fig. 6(A), lanes 3 and 5). The slightly reduced mobility of monomeric oxidized Ku likely also reflects cysteine oxidation, which may result in an intramolecular disulfide bridge as well as the formation of sulfenic and sulfinic acids. On treatment with oxidizing agent, we also expected to see a dimeric Ku of ~110 kDa if intermolecular disulfide bonds were to form. However, the presence of oligomeric species of 158 kDa is most likely owing to an anomalous migration of dimeric Ku as a trimer is difficult to reconcile with the dimeric Ku structure. We also note that the modest intermolecular disulfide bond formation is consistent with the model of Ku in which pairs of cysteine residues from each monomer are far apart and each pair of cysteines combines with histidine and aspartate from the other monomer to form a zinc site (Fig. 1); the limited intermolecular disulfide bond formation suggests that the bridge region is only modestly flexible. In contrast to untreated and bipyridyl-treated zinc-

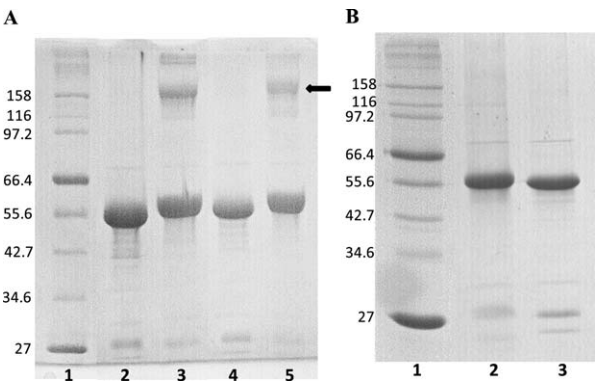

Figure 6. SDS-PAGE analysis of protein oxidation. (A) The effect of oxidizing and reducing agent on zinc-free native Ku and bipyridyl-treated Ku. Lane 1: molecular weight markers (identified at the left in kDa), lane 2: 5 μg of zinc-free native Ku with DTT (10 m*M*); lane 3: 5 μg of zinc-free native Ku with H_2O_2 (10 m*M*); lane 4: 5 μg of bipyridyl-treated native Ku with DTT (10 m*M*); lane 5: 5 μ*g* of bipyridyl-treated native Ku with H_2O_2 (10 m*M*). Oxidized species with lower electrophoretic mobility identified by an arrow. (B) The effect of oxidizing and reducing agent on zinc-bound native Ku. Lane 1: molecular weight markers (identified at the left in kDa); lane 2: 5 μg of zinc-bound native Ku with H_2O_2 (10 m*M*); lane 3: 5 μg of zinc-bound native Ku with DTT (10 m*M*).

Table I. *The Measurement of Free Sulfhydryl in Ku and Zinc-Bound Ku by DTNB Assay*

Protein sample	Free SH (μM)[a]	Relative free SH (%)[b]
Ku–Zn	5.8	5.9
Ku–Zn–H_2O_2 treated	5.0	5.0
Ku–bipyridyl	99.1	100
Ku–bipyridyl–H_2O_2 treated	12.5	12.6

[a] Free SH in Ku-bipyridyl (99.1 μM).
[b] Relative free SH (%) = free SH in sample × 100.
Abbreviation: SH, sulfhydryl.

free Ku, the exposure of zinc-bound native Ku to H_2O_2 did not produce higher oligomeric species, consistent with the interpretation that zinc coordinates with cysteine residues and prevents disulfide bond formation [Fig. 6(B)].

The proportion of free thiol was determined by modification with 5,5'-dithiobis-(2-nitrobenzoic acid (DTNB). Thiols in bipyridyl-treated zinc-free native Ku readily react with DTNB (almost quantitative conversion; Table I). In contrast, incubation with H_2O_2 reduces the relative content of free thiol to 12.6%, consistent with cysteine oxidation. Notably, zinc-bound native Ku contains only 5.9% of free thiol, suggesting that cysteines participate in metal coordination and that metal-binding prevents access to DTNB[15]; incubation of zinc-bound native Ku with H_2O_2 does not significantly reduce the content of free thiol (5.0%).

Zinc has little effect on DNA binding

The conformation of eukaryotic Ku is sensitive to redox conditions and its interaction with DNA is favored under reducing conditions.[16,17] Binding of *M. smegmatis* Ku to 37 bp DNA was examined using electrophoretic mobility shift assay (EMSA) (Supporting Information Fig. S3). Zinc-free Ku and zinc-bound Ku bound comparably in the absence of oxidizing and reducing agent, which shows that coordination of zinc did not affect the affinity for DNA (Table II). Under reducing conditions, the DNA binding affinity of zinc-free native and zinc-bound Ku increased modestly, as evidenced by an approximately twofold reduction in half-maximal saturation. Under oxidizing conditions, the affinity is similar to that observed for zinc-free native Ku (exposed to air) although Zn-bound Ku appeared modestly resistant to the effect of oxidant (Table II). These data show that the coordination of zinc to Ku has little effect on DNA binding and that DNA binding is only marginally attenuated by protein oxidation.

Table II. *Half-Maximal Saturation of DNA by Ku and Ku Mutant (KuC8891A)*

Proteins	Half-maximal saturation (nM)
Ku	8.6 ± 0.5
Ku–Zn	10.2 ± 1.7
KuC8891A	5.1 ± 0.9
KuC8891A–Zn	9.2 ± 0.6
Oxidizing conditions	
Ku	10.7 ± 0.4
Ku–Zn	7.8 ± 0.4
Reducing conditions	
Ku	4.7 ± 0.2
Ku–Zn	4.6 ± 0.2

DNA binding with mutant Ku (KuC8891A) showed half-maximal saturation at a concentration similar to that of zinc-free Ku and zinc-bound Ku under reducing conditions, indicating that the substitution of cysteines had no effect on DNA binding. Incubation of mutant Ku with zinc resulted in a modest decrease in DNA binding affinity as evidenced by an approximately twofold increase in the protein concentration required for half-maximal saturation (Table II). This is in contrast to the wild-type Ku, where Zn binding had no effect on DNA-binding affinity. Thus, zinc binding has a modest effect on DNA binding affinity of KuC8891A and is consistent with the results from the PAR assay that revealed zinc binding. However, the observation that zinc binding modestly reduces DNA-binding affinity of KuC8891C, but not wild-type Ku, suggests a distinct mode of zinc coordination. An alternative zinc-binding site only in KuC8891A would also be consistent with the DTNB assay, which implicates the cysteine residues in zinc binding to wild-type Ku.

Ku confers zinc tolerance

M. smegmatis Ku can bind zinc, and the stoichiometry of binding and ability of bound zinc to render cysteine inaccessible to covalent modification is consistent with binding to the predicted sites in the bridge region. However, the main effect of zinc binding appears to be a modest increase in thermal stability, with no significant effect on DNA binding. We therefore wondered about potential factors that might have exerted sufficient evolutionary pressure to retain the zinc sites in Ku from selected bacterial species. Although zinc is physiologically important, a high concentration of zinc is toxic, for example, because it competes with other metals for binding to the active sites of enzymes.[18] Therefore, homeostasis of zinc ion concentration is essential for mycobacterial species, many of which are environmental or pathogenic species that are exposed to assorted stress conditions, including the release of zinc from host mucosal surfaces in response to bacterial infection.[19]

If *M. smegmatis* Ku were to bind zinc as a mechanism to attenuate toxicity, we reasoned that it might be upregulated under the conditions of increased intracellular [Zn^{2+}]. The examination of the annotated *M. smegmatis* genome revealed that the gene encoding Ku (*MSMEG_5580*) is oriented

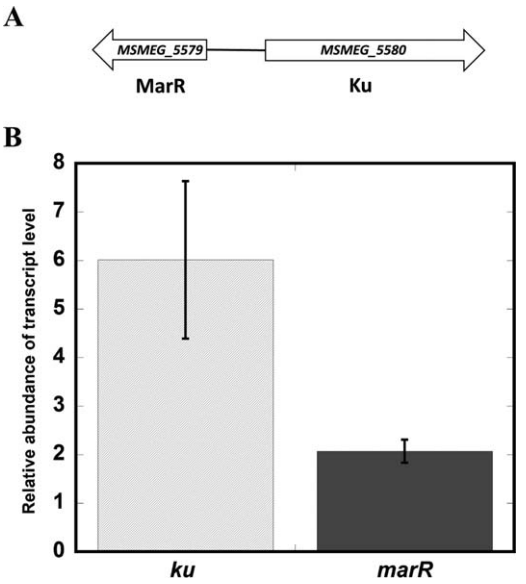

Figure 7. The effect of zinc on the expression of *M. smegmatis ku* and *marR*. (A) Genetic locus organization of *M. smegmatis ku* and *marR* genes. (B) Relative abundance of transcript levels of *ku* and *marR* genes after the addition of 2 m*M* of zinc. mRNA levels were measured with qRT-PCR and the relative abundance was calculated by the comparative C_T method with reference to transcript level of control. The error bars represent the S.D. of the three experiments.

divergently from a gene encoding a predicted multiple antibiotic resistance regulator (MarR) family protein (*MSMEG_5579*) [Fig. 7(A)]. This type of gene arrangement is not conserved in other mycobacterial species such as *M. tuberculosis*, *M. bovis*, *M. vanbaalenii*, and *M. gilvum*. The predicted MarR family transcriptional regulator is annotated as a member of the ubiquitous ArsR (or ArsR/SmtB) family of metalloregulators whose members act as metal sensors and derepress gene expression when metal ion becomes abundant.[20–23] Although ArsR proteins conserve the winged helix-turn-helix fold characteristic of MarR proteins, metal sites are not conserved and feature specificity for different metals and different coordination chemistry.[24] The general mechanism employed by ArsR family proteins is common for MarR family transcriptional regulators that are often divergently encoded from other genes or operons and respond to specific ligand binding by derepressing the gene(s) under their control (for review, see Refs. 25,26). The genomic locus encoding *M. smegmatis* Ku and the MarR homolog predicts upregulation of both genes on ligand binding to the transcription factor.

To assess whether the expression of these genes is altered by zinc, mid-log phase cultures of *M. smegmatis* were exposed to exogenous zinc (2 m*M*), a concentration chosen based on the reported minimum inhibitory concentration,[9] and the effect on transcription of both genes was determined. As evidenced by quantitative RT-PCR, growth in the presence of zinc led to an increase in the transcript level of both *marR* and *ku* genes by 2.1 ± 0.2- and 6.0 ± 1.6-fold, respectively [Fig. 7(B)]. This suggests that zinc functions as a ligand for the MarR homolog *in vivo*, causing derepression of *marR* and *ku* genes. Zinc homeostasis is controlled by mycobacterial transcription factors Zur and SmtB.[27] Zur controls zinc uptake in a Zn^{2+}-dependent manner, whereas *zur* expression is controlled by SmtB. SmtB represses the *smtB-zur* operon as well as the zinc-resistance determinant *zitA* in the absence of zinc; the examination of reporter constructs in *M. smegmatis* showed that the *zitA* promoter is activated when 10–100 μ*M* of Zn^{2+} is added to the culture.[27] The 2 m*M* zinc used to demonstrate the upregulation of *ku* would therefore be more than sufficient to induce this previously characterized zinc-resistance response, indicating that upregulation of *ku* occurs under previously established conditions of zinc toxicity. The mechanism of induction notwithstanding the significant increase in *ku* gene activity in response to zinc is consistent with the hypothesis that Ku may function to sequester excess metal.

The ability of *M. smegmatis* Ku to protect cells against toxic levels of zinc was tested in *E. coli*. Exposure to 1 m*M* of $ZnCl_2$ was sufficient to inhibit the growth of *E. coli* harboring plasmid without any insert or cells in which Ku expression was not induced. In contrast, cells induced for Ku overexpression (with expression confirmed by SDS-PAGE) continued to exhibit vigorous growth [Fig. 8(A)], consistent with Ku conferring protection against zinc toxicity. We also assessed the contribution of cysteine residues to zinc binding *in vivo* by performing the zinc toxicity test in *E. coli* transformed with plasmid carrying *M. smegmatis* Ku mutated for both of its cysteine residues. The result showed that exposure to 1 m*M* of $ZnCl_2$ inhibited the growth of *E. coli* in which the expression of mutant Ku was induced [Fig. 8(B)]. The inability of *E. coli* cells expressing mutant Ku to overcome zinc toxicity is consistent with the inference that KuC8891A employs a distinct mode of zinc coordination and that cysteine residues in wild-type Ku are involved in metal binding.

Conclusions

As predicted from sequence analyses, *M. smegmatis* Ku bound zinc (Fig. 3). The binding of zinc modestly enhanced protein stability, but it did not significantly affect DNA binding. This observation argues against a role for zinc binding in modulating the role of Ku in NHEJ. In addition, the interaction of *M. smegmatis* Ku with DNA was only modestly favored under reducing conditions (Supporting Information Fig. S3 and Table II), suggesting that Ku remains functional in NHEJ during oxidative stress.

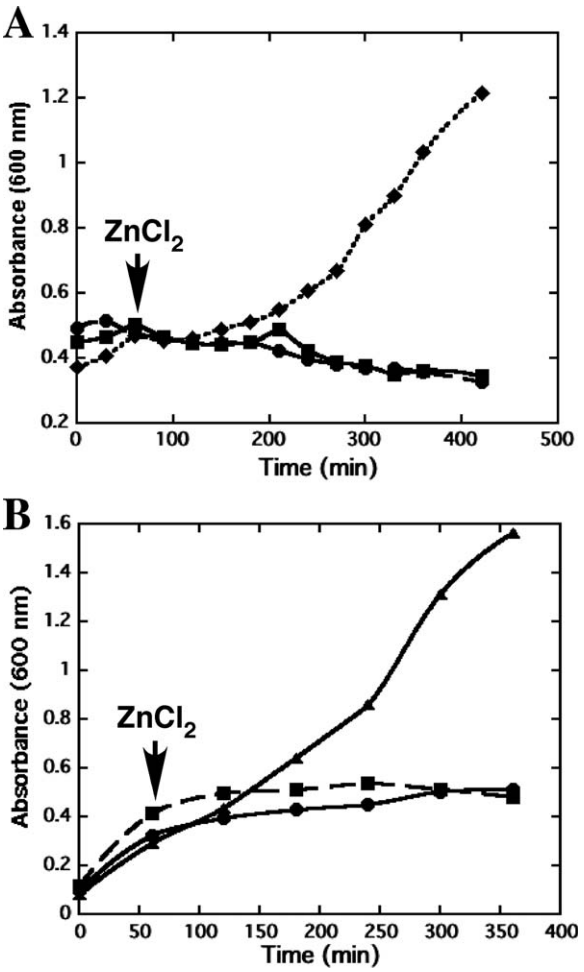

Figure 8. Growth of *E. coli* Rosetta cells in the presence of 1 m*M* of $ZnCl_2$. The horizontal axis shows time after the induction of protein expression. (A) Growth curve of cells induced for Ku expression (solid diamond); growth curve of uninduced cells (solid circle); growth curve of *E. coli* cells harboring plasmid without *ku* gene (solid square). (B) Growth curve of cells induced for Ku mutant expression in the presence of $ZnCl_2$ (solid circle); growth curve of uninduced cells in the presence of $ZnCl_2$ (solid square); growth curve of *E. coli* cells in the absence of $ZnCl_2$ (solid triangle). Addition of $ZnCl_2$ is marked with an arrow. Representative experiments are shown.

That thiols in zinc-free native Ku were fully accessible to covalent modification with DTNB, whereas only ~6% of thiols in zinc-bound Ku became modified (Table I) points to cysteines participating in metal coordination. This conclusion is substantiated by the ability of zinc binding to prevent protein oxidation (Fig. 6). The stoichiometry of zinc binding to Ku is consistent with the occupancy of two metal sites. Notably, the protection of *E. coli* from zinc toxicity was achieved only on the expression of wild-type Ku, not Ku in which both cysteines were replaced with alanine. We also note that DNA binding by wild-type Ku was unaffected by zinc, whereas the affinity of KuC8891A was modestly reduced by zinc. Based on these observations, we find it most likely that wild-type Ku indeed binds zinc at the computationally predicted sites that include the two cysteines, whereas the substitution of cysteine for alanine results in zinc coordination by alternate residues, possibly glutamates located near the cysteines in the DNA-binding loops. Adventitious coordination of metal by surface-exposed residues is not uncommon[28]; for example, the substitution of residues known from the crystal structure of the *Deinococcus radiodurans*-encoded DNA protection during starvation protein Dps-1 to coordinate metal does not abolish metal binding. Instead, neighboring residues were inferred to participate in metal binding.[29]

Zinc-binding sites within the Ku bridge-region have been retained only in Ku from select bacterial species (Fig. 2). However, the modest increase in thermal stability and protection against oxidative damage afforded by zinc binding does not appear to rationalize the evolutionary pressures to retain these sites, particularly considering that DNA binding is nearly unaffected by zinc binding or redox conditions. An alternate explanation is suggested by the observation that excess zinc is toxic and used by host cells as an antibacterial agent. For example, host macrophages release Zn^{2+} into phagosomes to limit the growth of *M. tuberculosis*.[30] Overexpression of Ku increased zinc tolerance of *E. coli* cells, and exposure to toxic levels of zinc increased transcription of the gene encoding Ku in *M. smegmatis* (Figs. 7 and 8). The Ku protein that was purified from *E. coli* in the presence of EDTA contained no zinc, and significant release of zinc was observed on the incubation of zinc-bound native Ku with PAR [Fig. 3(A)]; these observations may reflect that the affinity for zinc is lower than that generally observed for metalloproteins (which is often in the p*M* range). Consistent with this inference, we estimate that the affinity of Ku for zinc is ~0.8 n*M* (we consider this as an upper estimate, given that the His_6-tag appears to lower the affinity for zinc; Figs. 3 and 4). A lower affinity zinc binding would be consistent with a role for Ku in sequestering excess zinc as opposed to binding and depleting trace amounts of labile zinc. That zinc binding does not negatively affect known Ku function (i.e., DNA binding) is consistent with the evolutionary selection for, and retention of a secondary (moonlighting) function of Ku. Thus, zinc-binding sites in mycobacterial Ku may have been retained to provide additional protection against zinc toxicity by sequestering free Zn^{2+} without compromising normal Ku function in NHEJ repair of DNA double-strand breaks.

Protein moonlighting, in which a protein is performing more than one function, is generally believed to arise through an evolutionary process in which an apparently unrelated function is adopted in response to a selective pressure. Moonlighting proteins comprise their dual functions within one

polypeptide chain, that is, they have not arisen as a result of gene fusions, splice variations, and so forth (for review, see Refs. 31,32). In bacteria, such proteins often participate in cell-surface adhesion or stress responses; well-characterized examples include the glycolytic enzyme glyceraldehyde 3-phosphate dehydrogenase, which also mediates cell adhesion,[33] and the enzyme aconitase, which participates both in the citric acid cycle and in the iron homeostasis by binding an iron-responsive element in the untranslated regions of certain mRNAs and controlling their translation.[34] Protein moonlighting contributes to bacterial virulence; the ability of Mycobacterial Ku to sequester zinc would facilitate bacterial responses to environmental zinc exposure, including zinc produced by host macrophages following phagocytosis of bacteria.[30]

Materials and Methods

Preparation of Ku proteins

M. smegmatis Ku was purified and characterized as described earlier.[10,35] The two cysteine residues predicted to be part of the zinc-binding site were mutated by whole plasmid PCR amplification using Ku expression plasmid as template.[10] Both cysteines were replaced with alanine using mutagenic forward and reverse primers 5′-GTG **GCC** GAA GTC **GCC** GGC GAG-3′ and 5′-GCC **GGC** GAC TTC **GGC** CAC GC-3′ (mutated codons are indicated in boldface). The resultant PCR products were transformed into *E. coli* TOP10 cells, and integrity of the construct was confirmed by sequencing. *M. smegmatis* Ku and the mutant Ku proteins were purified with an N-terminal His_6-tag and characterized as described previously.[10] Briefly, the His_6-tagged Ku was purified by metal affinity chromatography and eluted from the column with imidazole. Purified Ku protein was dialyzed into a buffer containing 1 m*M* of EDTA and passed through a Q-Sepharose column.

Metal binding by Ku

To rule out zinc binding to the His_6-tag, the tag was cleaved by enterokinase and subsequently removed by incubation with Ni-agarose followed by centrifugation. Ku with and without His_6-tag was incubated with 50 m*M* of bipyridyl (metal chelator) for 30 min at 4°C to remove any metal from the protein. The bipyridyl-treated protein was then dialyzed overnight against buffer A (50 m*M* Tris-Cl [pH 8.0], 2 m*M* 2-mercaptoethanol, 100 m*M* NaCl, and 10% glycerol) at 4°C. The protein was then incubated with 1 m*M* of $ZnCl_2$ followed by overnight dialysis to remove excess metal. To denature, the protein was treated with 1% of SDS and heated at 90°C for 5 min. The samples were mixed with 100 μ*M* PAR in buffer A, and the absorbance from 320 to 625 nm was recorded using an Agilent 8453 spectrophotometer. All experiments were performed in duplicate.

The number of zinc ions bound to *M. smegmatis* Ku was determined by the PAR assay.[13] To ensure quantitative release of zinc, 0.5 μ*M* (monomer) of the protein was denatured by heating at 90°C for 5 min. Zinc-bound Ku without His_6-tag was mixed with 100 μ*M* of PAR in buffer A, and the absorbance was measured using an Agilent 8453 spectrophotometer. The quantity of zinc was determined from a standard curve, obtained by titrating PAR (100 μ*M*) with $ZnCl_2$ and measuring the absorbance at 500 nm. To estimate affinity, His_6-tagged protein (using Ku in which the lysine-rich C-terminal extension was truncated,[10] a modification not predicted to alter metal binding) was titrated into a solution of excess PAR (210 μ*M*) with 10 μ*M* of $ZnCl_2$ in buffer composed of 20 m*M* of Tris-HCl (pH 7.0) and 100 m*M* of KCl, and the decrease in absorbance at 500 nm was recorded after 2 min of incubation; the absorbance values were corrected for dilution. The K_d was estimated as described before, using a β_{PAR} of 2.2×10^{12} at pH 7.0.[11,36] All experiments were performed in duplicate.

Five micrograms of zinc-free Ku and zinc-bound Ku was incubated on ice for 30 min with 10 m*M* of H_2O_2 or 10 m*M* of dithiothreitol (DTT). The samples were then analyzed by SDS-PAGE.

Thermal stability assay

Zinc-free native Ku protein, bipyridyl-treated native Ku, or zinc-bound native Ku was diluted to 5 μ*M* in a buffer containing 50 m*M* of Tris (pH 8.0), 100 m*M* of NaCl, and 5× of SYPRO Orange (Invitrogen) as a reference fluorescent dye. The fluorescence emission was measured over a temperature range of 5–90°C in 1° increments for 40 s using an Applied Biosystems 7500 Real-Time PCR System (filter: SYBR green). Triplicate 50 μL samples were analyzed in a 96-well reaction plate. The total fluorescence yield measured was corrected using reactions without protein. The resulting data were analyzed with Sigma Plot 12 and the sigmoidal part of the curve was averaged for each triplicate. The averaged curves were subsequently fit to a four-parameter sigmoidal equation and the T_m values were determined. The S.D. values are derived from three replicates of an experiment.

Electrophoretic mobility shift assays

Oligodeoxyribonucleotides used to generate duplex DNA constructs were purchased and purified by denaturing polyacrylamide gel electrophoresis. One strand was ^{32}P-labeled at the 5′-end with phage T4 polynucleotide kinase. Equimolar amounts of complementary oligonucleotides were mixed, heated to 90°C, and cooled slowly to room temperature to form

duplex DNA. The concentrations of DNA were determined spectrophotometrically.

EMSAs were performed using 8% polyacrylamide gels (39:1 w/w acrylamide:bisacrylamide) in 0.5× of Tris/borate/EDTA (50 m*M* of Tris borate, and 1 m*M* of EDTA). Gels were prerun for 30 min at 175 V at room temperature before loading the samples. For measuring half-maximal saturation, 5 n*M* of ^{32}P-labeled 37-bp DNA was titrated with proteins, pretreated with either 10 m*M* of H_2O_2 or 10 mM of beta-mercaptoethanol in a total reaction volume of 10 μL in binding buffer (25 m*M* Tris-HCl [pH 8], 50 m*M* NaCl, 0.05% Triton X-100, and 2% v/v glycerol). The sequence of 37-bp DNA used was 5′-CCT AGG CTA CAC CTA CTC TTT GTA AGA ATT AAG CTT C-3′. The reactions were incubated at room temperature for 1 h and then loaded onto the gel with power on. After electrophoresis, gels were dried, and protein–DNA complexes and free DNA were quantified by phosphorimaging using software supplied by the manufacturer (Image Quant 1.1). Percentage complex formation was plotted as a function of protein concentrations and fitted to the Hill equation, $f = f_{max}$ ([Ku]^n/K_d^n) / (1+ ([Ku])^n/K_d^n) where [Ku] is the protein concentration, f is the fractional saturation, K_d reflects the half-maximal saturation, and n is the Hill coefficient. All bands corresponding to protein–DNA complexes, including the area between the fastest migrating complex and the free DNA, were considered as complex. Fits were performed using the program KaleidaGraph. The half-maximal saturation value is reported as the mean ± S.D. Experiments were performed in duplicate.

Growth of *E. coli* expressing *M. smegmatis* Ku

Two hundred milliliter of LB medium was inoculated with 1 mL of overnight starter culture of *E. coli* Rosetta cells (control) or Rosetta cells transformed with Ku or Ku mutant expression vector. Ku expression was induced with 1 m*M* of isopropyl-β-D-thiogalactopyranoside after inoculation. All cultures were allowed to grow for 60 min postinduction at 37°C followed by addition of $ZnCl_2$ to a final concentration of 1 m*M*. Absorbance at 600 nm was recorded for at least two cultures for each condition.

Measurement of cysteine oxidation

The oxidation state of zinc-free Ku and zinc-bound Ku was determined by adding Ellman's reagent, 5,5'-dithiobis-(2-nitrobenzoic acid) (DTNB), and measuring the formation of 5-thio-2-nitrobenzoic acid at 412 nm. A fresh solution of DTNB (12.5 m*M*) was prepared in 0.1 *M* of Tris buffer (pH 8.0). Ku (130 μ*M*) before and after H_2O_2 (10 m*M*) treatment was added to a mixture containing 100 μ*M* of DTNB, 2 m*M* of EDTA, and 6 *M* of urea. The amount of free thiol in Ku before and after treatment with H_2O_2 was calculated from a calibration curve generated by using appropriate concentrations of DTT.

In vivo gene expression in response to zinc

An overnight culture of *M. smegmatis* was diluted 1:100 in fresh Middlebrook 7H9 media and challenged with zinc at a final concentration of 2 m*M*, which is above the reported minimal inhibitory concentration of 1.5 m*M* for *M. smegmatis* mc^{2}155.[37] Cells were harvested by centrifugation when the cultures reached an optical density of ~0.5 at 600 nm, followed by isolation of total RNA with Illustra RNAspin Mini Isolation Kit (GE Healthcare). cDNA was prepared from 300 ng of total RNA with AMV reverse transcriptase according to the methods described by Sambrook and Russell.[38] and quantitative PCR was carried out with a Applied Biosystems 7500 Real Time PCR system. DNA representing *ku* and *marR* and the internal control gene *rrsA* was amplified with specific primers using SYBR green 1 fluorescence as a reporter of amplification. Isolated RNA samples were included in all experiments as a control for DNA contamination. For each sample, melting curves were recorded and samples were subsequently run on an agarose gel to confirm the purity of the products. Necessary controls and validations were carried out before applying the comparative C_T ($2^{-\Delta\Delta C_T}$) method for data analysis.[39]

Acknowledgments

The authors thank Marcia Newcomer for the use of her spectrophotometer.

References

1. Doherty AJ, Jackson SP, Weller GR (2001) Identification of bacterial homologues of the Ku DNA repair proteins. FEBS Lett 500:186–188.
2. Featherstone C, Jackson SP (1999) Ku, a DNA repair protein with multiple cellular functions? Mutat Res 434:3–15.
3. Yoo S, Dynan WS (1999) Geometry of a complex formed by double strand break repair proteins at a single DNA end: recruitment of DNA-PKcs induces inward translocation of Ku protein. Nucleic Acids Res 27:4679–4686.
4. Weller GR, Kysela B, Roy R, Tonkin LM, Scanlan E, Della M, Devine SK, Day JP, Wilkinson A, d'Adda di Fagagna F, Devine KM, Bowater RP, Jeggo PA, Jackson SP, Doherty AJ (2002) Identification of a DNA nonhomologous end-joining complex in bacteria. Science 297:1686–1689.
5. Aravind L, Koonin EV (2001) Prokaryotic homologs of the eukaryotic DNA-end-binding protein Ku, novel domains in the Ku protein and prediction of a prokaryotic double-strand break repair system. Genome Res 11:1365–1374.
6. Shuman S, Glickman MS (2007) Bacterial DNA repair by non-homologous end joining. Nat Rev Microbiol 5: 852–861.

7. Downs JA, Jackson SP (2004) A means to a DNA end: the many roles of Ku. Nat Rev Mol Cell Biol 5:367–378.
8. Walker JR, Corpina RA, Goldberg J (2001) Structure of the Ku heterodimer bound to DNA and its implications for double-strand break repair. Nature 412:607–614.
9. Krishna SS, Aravind L (2010) The bridge-region of the Ku superfamily is an atypical zinc ribbon domain. J Struct Biol 172:294–299.
10. Kushwaha AK, Grove A (2013) C-terminal low-complexity sequence repeats of *Mycobacterium smegmatis* Ku modulate DNA binding. Biosci Rep 33:175–184.
11. Walkup GK, Imperiali B (1997) Fluorescent chemosensors for divalent zinc based on zinc finger domains. Enhanced oxidative stability, metal binding affinity, and structural and functional characterization. J Am Chem Soc 119:3443–3450.
12. Hogbom M, Ericsson UB, Lam R, Bakali HM, Kuznetsova E, Nordlund P, Zamble DB (2005) A high throughput method for the detection of metalloproteins on a microgram scale. Mol Cell Proteomics 4:827–834.
13. Hunt JB, Neece SH, Ginsburg A (1985) The use of 4-(2-pyridylazo)resorcinol in studies of zinc release from *Escherichia coli* aspartate transcarbamoylase. Anal Biochem 146:150–157.
14. Vedadi M, Niesen FH, Allali-Hassani A, Fedorov OY, Finerty PJ, Jr, Wasney GA, Yeung R, Arrowsmith C, Ball LJ, Berglund H, Hui R, Marsden BD, Nordlund P, Sundstrom M, Weigelt J, Edwards AM (2006) Chemical screening methods to identify ligands that promote protein stability, protein crystallization, and structure determination. Proc Natl Acad Sci USA 103:15835–15840.
15. Griep MA, Lokey ER (1996) The role of zinc and the reactivity of cysteines in *Escherichia coli* primase. Biochemistry 35:8260–8267.
16. Bennett SM, Neher TM, Shatilla A, Turchi JJ (2009) Molecular analysis of Ku redox regulation. BMC Mol Biol 10:86.
17. Lehman JA, Hoelz DJ, Turchi JJ (2008) DNA-dependent conformational changes in the Ku heterodimer. Biochemistry 47:4359–4368.
18. Blencowe DK, Morby AP (2003) Zn(II) metabolism in prokaryotes. FEMS Microbiol Rev 27:291–311.
19. Crane JK, Byrd IW, Boedeker EC (2011) Virulence inhibition by zinc in shiga-toxigenic *Escherichia coli*. Infect Immun 79:1696–1705.
20. Busenlehner LS, Pennella MA, Giedroc DP (2003) The SmtB/ArsR family of metalloregulatory transcriptional repressors: structural insights into prokaryotic metal resistance. FEMS Microbiol Rev 27:131–143.
21. Chauhan S, Kumar A, Singhal A, Tyagi JS, Krishna Prasad H (2009) CmtR, a cadmium-sensing ArsR-SmtB repressor, cooperatively interacts with multiple operator sites to autorepress its transcription in *Mycobacterium tuberculosis*. FEBS J 276:3428–3439.
22. Wu J, Rosen BP (1991) The ArsR protein is a trans-acting regulatory protein. Mol Microbiol 5:1331–1336.
23. Arunkumar AI, Campanello GC, Giedroc DP (2009) Solution structure of a paradigm ArsR family zinc sensor in the DNA-bound state. Proc Natl Acad Sci USA 106:18177–18182.
24. Campanello GC, Ma Z, Grossoehme NE, Guerra AJ, Ward BP, Dimarchi RD, Ye Y, Dann CE, 3rd, Giedroc DP (2013) Allosteric inhibition of a zinc-sensing transcriptional repressor: insights into the arsenic repressor (ArsR) family. J Mol Biol 425:1143–1157.
25. Perera IC, Grove A (2010) Molecular mechanisms of ligand-mediated attenuation of DNA binding by MarR family transcriptional regulators. J Mol Cell Biol 2:243–254.
26. Grove A (2013) MarR family transcription factors. Curr Biol 23:R142–R143.
27. Riccardi G, Milano A, Pasca MR, Nies DH (2008) Genomic analysis of zinc homeostasis in *Mycobacterium tuberculosis*. FEMS Microbiol Lett 287:1–7.
28. Xiao ZG, Wedd AG (2010) The challenges of determining metal-protein affinities. Nat Prod Rep 27:768–789.
29. Nguyen KH, Grove A (2012) Metal binding at the *Deinococcus radiodurans* Dps-1 N-terminal metal site controls dodecameric assembly and DNA binding. Biochemistry 51:6679–6689.
30. Botella H, Peyron P, Levillain F, Poincloux R, Poquet Y, Brandli I, Wang C, Tailleux L, Tilleul S, Charriere GM, Waddell SJ, Foti M, Lugo-Villarino G, Gao Q, Maridonneau-Parini I, Butcher PD, Castagnoli PR, Gicquel B, de Chastellier C, Neyrolles O (2011) Mycobacterial p(1)-type ATPases mediate resistance to zinc poisoning in human macrophages. Cell Host Microbe 10:248–259.
31. Jeffery CJ (2009) Moonlighting proteins—an update. Mol BioSyst 5:345–350.
32. Kainulainen V, Korhonen TK (2014) Dancing to another tune-adhesive moonlighting proteins in bacteria. Biology 3:178–204.
33. Pancholi V, Fischetti VA (1992) A major surface protein on group A streptococci is a glyceraldehyde-3-phosphate-dehydrogenase with multiple binding activity. J Exp Med 176:415–426.
34. Banerjee S, Nandyala AK, Raviprasad P, Ahmed N, Hasnain SE (2007) Iron-dependent RNA-binding activity of *Mycobacterium tuberculosis* aconitase. J Bacteriol 189:4046–4052.
35. Kushwaha AK, Grove A (2013) *Mycobacterium smegmatis* Ku binds DNA without free ends. Biochem J 456:275–282.
36. Atanassova A, Zamble DB (2005) *Escherichia coli* HypA is a zinc metalloprotein with a weak affinity for nickel. J Bacteriol 187:4689–4697.
37. Grover A, Sharma R (2006) Identification and characterization of a major Zn(II) resistance determinant of *Mycobacterium smegmatis*. J Bacteriol 188:7026–7032.
38. Sambrook J, Russell DW (2001) Molecular cloning: a laboratory manual. Cold Spring Harbor, NY: Cold Spring Harbor Laboratory.
39. Schmittgen TD, Livak KJ (2008) Analyzing real-time PCR data by the comparative C_T method. Nat Protoc 3: 1101–1108.